Kinetics Studies of Aqueous Phase Reactions of Cl Atoms and Cl_2^- Radicals with Organic Sulfur Compounds of Atmospheric Interest

Lei Zhu,[†,‡] J. Michael Nicovich,[§] and Paul H. Wine*[,‡,§]

School of Earth and Atmospheric Sciences and School of Chemistry and Biochemistry, Georgia Institute of Technology, Atlanta, Georgia 30332

Received: December 14, 2004; In Final Form: March 8, 2005

A laser flash photolysis−long path UV−visible absorption technique has been employed to investigate the kinetics of aqueous phase reactions of chlorine atoms (Cl) and dichloride radicals (Cl_2^-) with four organic sulfur compounds of atmospheric interest, dimethyl sulfoxide (DMSO; $CH_3S(O)CH_3$), dimethyl sulfone ($DMSO_2$; $CH_3(O)S(O)CH_3$), methanesulfinate (MSI; $CH_3S(O)O^-$), and methanesulfonate (MS; $CH_3(O)S(O)O^-$). Measured rate coefficients at $T = 295 \pm 1$ K (in units of M^{-1} s^{-1}) are as follows: Cl + DMSO, $(6.3 \pm 0.6) \times 10^9$; Cl_2^- + DMSO, $(1.6 \pm 0.8) \times 10^7$; Cl + $DMSO_2$, $(8.2 \pm 1.6) \times 10^5$; Cl_2^- + $DMSO_2$, $(8.2 \pm 5.5) \times 10^3$; Cl_2^- + MSI, $(8.0 \pm 1.0) \times 10^8$; Cl + MS, $(4.9 \pm 0.6) \times 10^5$; Cl_2^- + MS, $(3.9 \pm 0.7) \times 10^3$. Reported uncertainties are estimates of accuracy at the 95% confidence level and the rate coefficients for MSI and MS reactions with Cl_2^- are corrected to the zero ionic strength limit. The absorption spectrum of the DMSO−Cl adduct is reported; peak absorbance is observed at 390 nm and the peak extinction coefficient is found to be 5760 M^{-1} cm^{-1} with a 2σ uncertainty of ±30%. Some implications of the new kinetics results for understanding the atmospheric sulfur cycle are discussed.

Introduction

It has been proposed that dimethyl sulfide (DMS; CH_3SCH_3) oxidation in the marine atmosphere may play an important role in modifying or regulating global climate because several sulfur-containing species produced from the free radical initiated oxidation of gas-phase DMS are water soluble and could be involved in formation and growth of atmospheric aerosols.[1−6] Important stable water-soluble intermediates that are generated via atmospheric DMS oxidation include dimethyl sulfoxide (DMSO; $CH_3S(O)CH_3$), dimethyl sulfone ($DMSO_2$; $CH_3(O)S(O)CH_3$), methanesulfinic acid (MSIA; $CH_3S(O)OH$), methanesulfonic acid (MSA; $CH_3(O)S(O)OH$), SO_2, and sulfuric acid (H_2SO_4; $HO(O)S(O)OH$).[7] If given time to equilibrate with the atmospheric condensed phase, all of the above DMS oxidation products are partitioned partially or primarily (almost exclusively in the cases of MSA and H_2SO_4) into the condensed phase.[3,5,6,8−15] Both model studies and field observations have demonstrated that condensed phase transformations are potentially important in the atmospheric sulfur cycle and in affecting the physicochemical properties of aerosols and cloud/rain droplets, because through these aqueous phase reactions relatively volatile species, i.e., SO_2 and DMSO, are converted into relatively nonvolatile species, i.e., MS (the deprotonated form of MSA) and sulfate, which stay in particles as cloud droplets evaporate, thus contributing to particle growth.

Unfortunately, the available kinetics database for aqueous phase reactions of organic sulfur compounds with important atmospheric oxidants is rather limited. The most studied reactions are those with OH, a key gas phase and aqueous phase atmospheric oxidant. Kinetics data for the OH + DMSO reaction reported in our recent study[16] are in good agreement with most previous studies,[17−21] suggesting a room-temperature rate coefficient in the range $(6.0 \pm 1.0) \times 10^9$ M^{-1} s^{-1}. The room-temperature rate coefficient for the OH + $DMSO_2$ reaction reported in our recent study[16] is lower than the value reported by Milne et al.[20] by about a factor of 2. Three studies of the MSI + OH reaction[21−23] are in reasonable agreement and indicate that this is a very fast reaction with a room-temperature rate coefficient near the diffusion-controlled limit (MSI is the deprotonated form of MSIA). The room-temperature rate coefficient for the potentially atmospherically important OH + MS reaction reported in our recent study[16] agrees well with the lowest[24] of three literature values[20,24,25] indicating that this reaction is rather slow with a rate coefficient of about $(1.1 \pm 0.2) \times 10^7$ M^{-1} s^{-1}. Our recent kinetics study of SO_4^- reactions with organic sulfur compounds[26] showed a similar reactivity trend to that observed for OH radicals, and supports the idea that fast reactions of SO_4^- with the S(IV) species DMSO and MSI make nonnegligible contributions to the oxidation of these species in the atmospheric aqueous phase.

The only kinetics studies of reactions of organic sulfur compounds with the two important atmospheric aqueous phase radicals Cl and Cl_2^- are one study of Cl_2^- + DMSO in aqueous solution[27] and one study of Cl + DMSO in CCl_4 solvent;[28] the reported rate coefficients (in units of M^{-1} s^{-1}) are 1.2×10^7 and 7.0×10^9, respectively. In marine boundary layer cloud droplets, typical Cl_2^- and Cl^- concentrations are $\sim 10^{-11}$ M[29] and 10^{-5}−10^{-4} M,[30,31] respectively, so typical Cl concentrations are 7×10^{-13}−7×10^{-12} M (based on the known equilibrium constant[32] for $Cl + Cl^- \; Cl_2^-$). In deliquescent sea-salt particles where chloride concentrations are 5−6 orders of magnitude higher than in cloud droplets, Cl concentrations are negligible. The high redox potentials of $Cl_2^-/2Cl^-$ ($E° = +2.2$ V) and Cl/Cl^- ($E° = +2.42$ V)[33−35] make these radicals very efficient

* Address correspondence to this author. Phone: +1 (404) 894-3425. Fax: +1 (404) 894-5638. E-mail: pw7@prism.gatech.edu.
† Present address: NOAA Aeronomy Laboratory, 325 Broadway, R/AL 2, Boulder, CO 80305-3328.
‡ School of Earth and Atmospheric Sciences.
§ School of Chemistry and Biochemistry.

10.1021/jp044306u CCC: $30.25
Published on Web 04/06/2005

oxidants in the atmospheric condensed phase. Considering their reactivity and relatively high concentrations, Cl and Cl_2^- could play significant roles as oxidants for organic sulfur compounds in marine atmospheric aerosols and cloud droplets.

As the third part of a series of kinetics studies of potentially important atmospheric condensed phase reactions of organic sulfur species, the present study employs a laser flash photolysis (LFP)−long path UV−visible absorption (LPA) technique to carry out investigations of aqueous phase reactions of Cl and Cl_2^- radicals with four organic sulfur compounds of atmospheric interest, i.e., DMSO, $DMSO_2$, MSI, and MS.

Experimental Technique

The LFP−LPA technique involves coupling radical production by laser flash photolysis of aqueous $S_2O_8^{2-}/Cl^-/R$ (R = DMSO, $DMSO_2$, MSI, or MS) solutions with sensitive time-resolved detection of $Cl \rightleftarrows Cl_2^-$ radicals by multipass absorption spectroscopy at $\lambda = 340$ nm. A detailed description and a schematic diagram of the experimental apparatus have been published elsewhere.[26] Important features of the methodology include the following: (1) reactive intermediates are probed in "real-time", i.e., on time scales corresponding to their lifetimes under the experimental conditions employed (10^{-6}−10^{-2} s), and (2) very low radical concentrations are employed, thereby eliminating many potential side reactions that could seriously complicate the interpretation of kinetic data. The photolysis laser employed in this study was a Lambda Physik Compex 102 excimer laser operating with a KrF gas fill ($\lambda = 248$ nm, pulse width = 25 ns). The laser fluence at the entrance to the reaction cell was typically 1.5×10^{16} photons cm^{-2} $pulse^{-1}$. In all experiments White cell mirrors[36] were adjusted to allow at least 34 passes of the probe radiation from a cw xenon arc lamp through the region of the reactor irradiated by the laser, giving an absorption path length of ∼85 cm. With an electronic time constant of 1 μs, the detection limit is about 0.03% absorption (64 flashes averaged); assuming a peak (340 nm) Cl_2^- extinction coefficient[32,37] of ∼8800 M^{-1} cm^{-1}, the detection limit of Cl_2^- under the conditions employed in this study is estimated to be $\sim 2 \times 10^{-10}$ M. The photolysis laser traversed the reactor at right angles to the probe radiation. The path length of solution traversed by the photolysis laser was 4.3 cm, with approximately the middle 2 cm of this path being probed. As discussed below, radicals were generated by laser flash photolysis of $S_2O_8^{2-}$ at 248 nm. The extinction coefficient for $S_2O_8^{2-}$ at 248 nm is 26 M^{-1} cm^{-1},[38] and $S_2O_8^{2-}$ concentrations employed in this study ranged from 5×10^{-5} to 5×10^{-4} M; hence, all solutions were optically thin toward laser radiation, i.e., gradients in radical concentrations across the probed region were negligible. The concentration of SO_4^- radicals generated by the laser pulse was in the range 10^{-8}−10^{-7} M in a majority of experiments.

Solutions were made with Millipore Milli-Q water (resistance greater than 15 megohms), and all chemicals used in this study were ACS reagent grade or better. The stated minimum purities of the chemicals are as follows: sodium chloride, 99.999%; sodium persulfate, 98%; sodium methanesulfinate, 97%; sodium methanesulfonate, 98% (aqueous solutions were colorless); $DMSO_2$, 98%; DMSO, 99.9%. These chemicals were used without further purification. All solutions were unbuffered with pH in the 5−6 range, and air saturated. During the experiments, solutions were pumped through the 55 cm^3 reactor without recycling. Typically, the laser repetition rate and the solution flow rate were adjusted to be 0.03 Hz and 2.5 cm^3 s^{-1}, respectively, so that no aliquot of solution was subjected to more than one laser flash. In most experiments, solutions were used immediately after preparation, although kinetics results for all reactions were found to be unaffected by allowing the solution to sit at room temperature overnight before being used in an experiment. Kinetics results were also unaffected by switching from air-saturated to N_2-saturated solutions. All experiments were carried out at room temperature, $T = 295 \pm 1$ K.

Results and Discussion

Kinetics of $Cl \rightleftarrows Cl_2^-$ Degradation in Water. The photolysis of persulfate anions ($S_2O_8^-$) at 248 nm results in production of sulfate radicals (SO_4^-) with high yield:[32,38]

$$S_2O_8^{2-} + h\nu\ (248\ nm) \rightarrow 2SO_4^- \qquad (R1)$$

For the relatively low $S_2O_8^{2-}$ and SO_4^- levels employed in this study, when chloride ions (Cl^-) are present in the system at concentrations greater than 5×10^{-5} M, self-reaction and the reaction with $S_2O_8^-$ are negligible SO_4^- loss processes; under such conditions, SO_4^- radicals react virtually exclusively with Cl^- via R2, followed by rapid equilibration of Cl and Cl_2^- radicals[38−43] via R3 and R−3:

$$SO_4^- + Cl^- \rightarrow SO_4^{2-} + Cl \qquad (R2)$$

$$Cl + Cl^- \rightleftarrows Cl_2^- \qquad (R3, R-3)$$

It is well-established in the literature[32,40,44−48] that the Cl and Cl_2^- radicals undergo the following additional reactions in aqueous solution:

$$Cl + H_2O \rightarrow HOCl^- + H^+ \qquad (R4)$$

$$Cl_2^- + H_2O \rightarrow HOCl^- + H^+ + Cl^- \qquad (R5)$$

$$Cl_2^- + Cl_2^- \rightarrow Cl_2 + 2Cl^- \qquad (R6)$$

Although evidence for the occurrence of reactions of Cl and Cl_2^- with $S_2O_8^{2-}$ is reported in the literature,[32] these reactions are unimportant at the low $S_2O_8^{2-}$ concentrations employed in this study. Even though the Cl_2^- self-reaction (R6) is quite fast ($k \sim 10^9$ M^{-1} s^{-1}),[49] this reaction is unimportant under most experimental conditions employed in this study because of the low radical concentrations employed. However, as discussed below, we find that the $Cl_2^- + H_2O$ reaction (R5) is extremely slow, so some contribution from R6 to the very slow decays measured at high Cl^- concentrations (when organic sulfur compounds are absent in the system) is likely. The observed kinetics of $Cl \rightleftarrows Cl_2^-$ reactions with organic sulfur compounds, which are discussed in a later section, and which are the major emphasis of this work, are unaffected by interference from R6.

Figure 1 shows typical absorbance temporal profiles observed at 340 nm in the $Cl^-/S_2O_8^{2-}/h\nu$ system. Both Cl_2^- and Cl absorb at 340 nm with extinction coefficients of ∼8800 M^{-1} cm^{-1} [32,37] and ∼3700 M^{-1} cm^{-1},[50] respectively. Within the Cl^- concentration range studied (5×10^{-5} to 0.25 M), the absorbance rise times are short when compared to the decay times; hence, a simple first-order kinetics analysis method could be employed to evaluate the decay times. We find that the pseudo-first-order loss rate of $Cl \rightleftarrows Cl_2^-$ radicals, k'_0 (primed rate coefficients are pseudo-first order), increases from <100 s^{-1} to ∼8000 s^{-1} as the Cl^- concentration decreases from 0.25 M to 1.0×10^{-4} M. Under the experimental conditions employed, i.e., over the Cl^- concentration range studied, R3 is fast enough[32,44,50] that equilibrium between Cl and Cl_2^- is maintained as the radicals

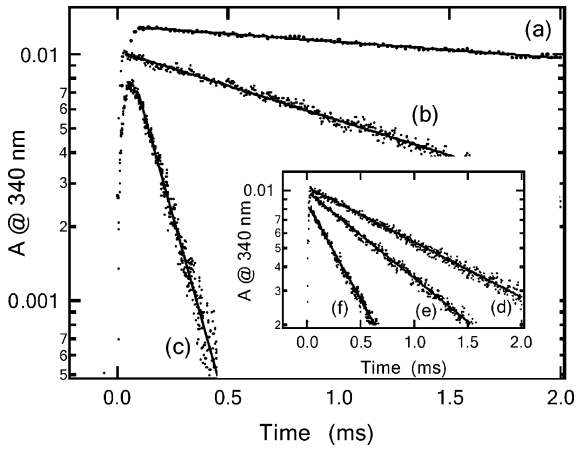

Figure 1. Absorbance temporal profiles detected at 340 nm in the $S_2O_8^{2-}/Cl^-/h\nu$ systems. Experimental conditions: $[S_2O_8^{2-}] = 1.45 \times 10^{-5}$ M, [R] = 0, $[Cl^-]$ = (a) 1.0×10^{-2}, (b) 1.0×10^{-3}, and (c) 1.0×10^{-4} M for the main plot; $[S_2O_8^{2-}] = 1.45 \times 10^{-5}$ M, $[Cl^-] = 1.0 \times 10^{-3}$ M, [DMSO] = (d) 0, (b) 5.67×10^{-6}, and (c) 2.83×10^{-5} M for the inset plot. The solid lines are obtained from linear least-squares analyses and give the following first-order decay rates (in units of s^{-1}): (a) 145, (b) 1040, (c) 7850, (d) 850, (e) 1060, and (f) 2590.

decay. Therefore, the chemistry of both Cl and Cl_2^- radicals contributes to k'_0 and the fraction of each radical in the reaction mixture is determined by K_3 and $[Cl^-]$. When $[Cl^-]$ is relatively low, Cl concentrations are substantial and R4 is the dominant pathway for radical loss. At higher $[Cl^-]$, the Cl_2^-/Cl concentration ratio becomes very large and, at some point, R5 becomes a more important loss process than R4 for the radical pool. Experiments at high Cl^- concentrations, where very slow decays were observed, were carried out with particularly low radical concentrations ($\sim 10^{-8}$ M) to minimize the contribution from R6 to the observed kinetics; however, it appears that R5 is so slow that some contribution from R6 could not be avoided. Under the assumptions (a) that equilibrium between Cl and Cl_2^- is maintained throughout the decay of the radical pool and (b) that R4 and R5 are the only important processes for destruction of $Cl \rightleftarrows Cl_2^-$ radicals, k'_0 can be expressed as follows:

$$k'_0 = \alpha k'_4 + \beta k'_5 \qquad (1)$$

In eq 1, α and β are fractions of Cl and Cl_2^- radicals defined as $\alpha = [Cl]/([Cl] + [Cl_2^-])$ and $\beta = [Cl_2^-]/([Cl] + [Cl_2^-])$. Hence eq 1 can be rewritten as:

$$k'_0 = \frac{1}{1 + K_3[Cl^-]} k'_4 + \frac{K_3[Cl^-]}{1 + K_3[Cl^-]} k'_5 \qquad (2)$$

A plot of k'_0 as a function of $[Cl^-]$ is shown in Figure 2. The solid curve in Figure 2 is obtained from the best fit of k'_0 vs $[Cl^-]$ data to eq 2 with k'_4, k'_5, and K_3 as adjustable parameters. K_3 obtained from our fit agrees well with the frequently cited literature value of 1.4×10^5 M^{-1}.[32,47] The rate coefficients $k'_4 = (1.4 \pm 0.2) \times 10^5$ s^{-1} and $k'_5 = 40 \pm 20$ s^{-1} were obtained from the fit, where the uncertainties are 2σ and represent precision only. As compared in Table 2, our value of k'_4 agrees well with the studies from Klaning and Wolff[44] and Yu et al.,[32] but it is more than 40% lower than the values reported by Buxton et al.[47] and McElroy.[40] Our value of k'_5 is slower than most literature values,[32,40,47,51,52] but it is comparable to $2k_6[Cl_2^-]$ estimated by using the experimental $[Cl_2^-]$ of $\sim 10^{-8}$ M and the literature value $k_6 \sim 10^9$ M^{-1} s^{-1}.[32,40,49,53,54] Hence, in disagreement with several published values,[32,40,47] our results

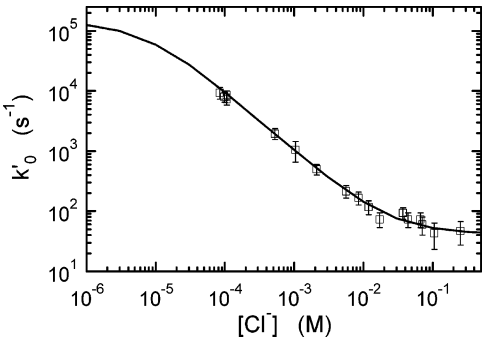

Figure 2. Plot of measured first-order decay rates (k'_0) versus $[Cl^-]$ in the $S_2O_8^{2-}/Cl^-/h\nu$ system. The solid curve is the best fit of the data to eq 3 in the text, and gives the parameters $k'_4 = (1.4 \pm 0.1) \times 10^5$ s^{-1}, $k'_5 = 40 \pm 20$ s^{-1}, and $K_3 = (1.4 \pm 0.1) \times 10^5$ M^{-1}; uncertainties are 2σ and represent precision only.

support a very small value for the $Cl_2^- + H_2O$ rate coefficient. Taking the value 40 ± 20 s^{-1} obtained from the data in Figure 2 as a conservative upper limit, we report $k'_5 < 60$ s^{-1}; however, we point out that k'_5 is probably significantly smaller than the reported limit, since reaction with background impurities and R6 both probably contribute to the observed slow loss of Cl_2^-.

The different radical concentrations employed are likely to be responsible for discrepancies in the $Cl_2^- + H_2O$ rate coefficients reported in the literature. In the study of McElroy[40] the concentration of Cl_2^- was $>10^{-6}$ M, i.e., about 2 orders of magnitude higher than that employed in our study; the reported Cl_2^- decay rate of 1300 s^{-1} was attributed to R5 but was probably dominated by R6. In the recent study of Yu et al.,[32] a much lower Cl_2^- concentration of $\sim 10^{-7}$ M was employed and a rate coefficient of <100 s^{-1} for $Cl_2^- + H_2O$ was reported.

Kinetics of $Cl \rightleftarrows Cl_2^-$ Reactions with DMSO, $DMSO_2$, MSI, and MS. After the introduction of sulfur species, R (R = DMSO, $DMSO_2$, MSI, or MS), into the system, the detected $Cl \rightleftarrows Cl_2^-$ decay rate is enhanced due to the reactions of $Cl \rightleftarrows Cl_2^-$ with the sulfur species. The inset in Figure 1 shows a set of absorbance temporal profiles observed when varying concentrations of DMSO are added to a 10^{-3} M $[Cl^-]$ solution; as typified by these data, at constant $[Cl^-]$ and $[S_2O_8^{2-}]$, the pseudo-first-order decay rate, k'_{DMSO}, increases with increasing DMSO concentration. As shown in panel a of Figure 3, plots of $k'_{DMSO} - k'_0$ vs [DMSO] are linear, and their slope gives the second-order rate coefficient, k_{DMSO}. Using this method, second-order rate coefficients (k_R) for DMSO, $DMSO_2$, MSI, and MS reactions at different Cl^- concentrations were determined; these second-order rate coefficients are, of course, "composite" rate coefficients that contain contributions from both Cl + R and Cl_2^- + R. In Figure 3, plots of measured $k'_R - k'_0$ vs [R] for R = DMSO, $DMSO_2$, MSI, and MS at different Cl^- concentrations are compared. As discussed above, k'_0 is a function of $[Cl^-]$, so it was subtracted from k'_R for a better data comparison. As typified by the data shown in Figure 3, very good linear relationships between $k'_R - k'_0$ and [R] were observed for all Cl^- concentrations studied for the $DMSO_2$, MSI, and MS reactions. The second-order rate coefficients (k_R) obtained from linear-least-squares fits of the $k'_R - k'_0$ vs [R] data for the DMSO, $DMSO_2$, MSI, and MS reactions are summarized in Table 1. For the $DMSO_2$ and MS reactions (panels b and d in Figure 3) as well as the more complex DMSO reaction that is discussed separately below (panel a in Figure 3), the values for k_R were found to decrease with increasing $[Cl^-]$, which is expected because, as mentioned above, the following two

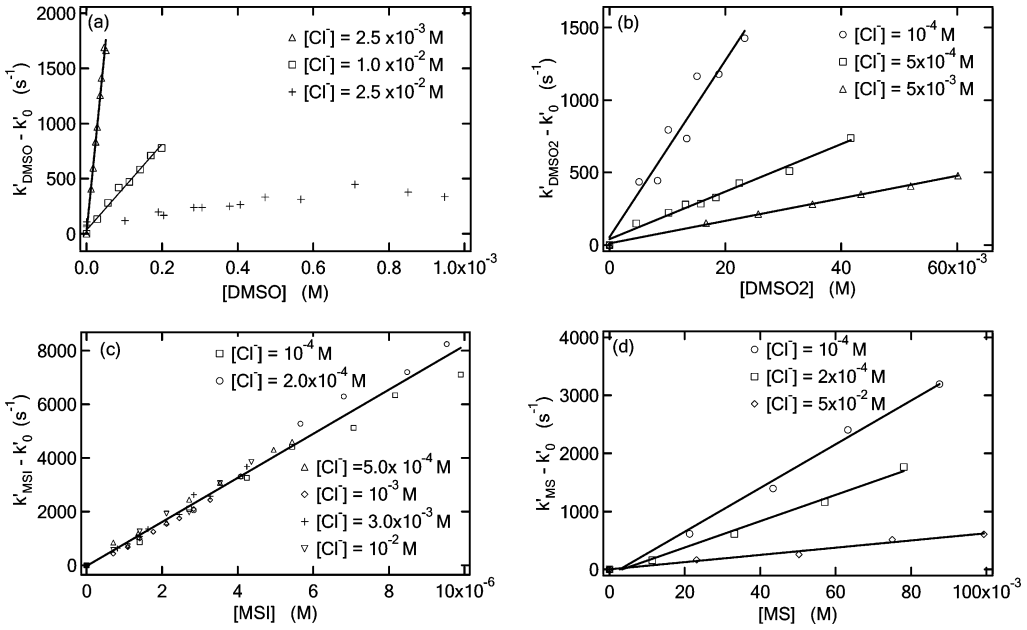

Figure 3. Plots of $k'_R - k'_0$ vs R for R = [DMSO] (a), [DMSO2] (b), [MSI] (c), and [MS] (d) at different [Cl⁻]. The solid lines are obtained from linear least-squares analyses and give rate coefficients that are summarized in Table 1.

TABLE 1: Summary of Second-Order Rate Coefficients, k_R, for the DMSO, $DMSO_2$, MSI, MS, and H_2O Reactions with $Cl \rightleftarrows Cl_2^-$ at All Studied Cl^- Concentrations[a]

	k_R ($M^{-1} s^{-1}$)				
[Cl⁻] (M)	water	R = DMSO	MSI	DMSO2	MS
1×10^{-4}	150	3.88×10^8	7.45×10^8	61100	37600
2.0×10^{-4}	75				22600
2.5×10^{-4}	64	1.93×10^8	8.86×10^8		
5×10^{-4}	37	9.56×10^7	8.41×10^8	16400	
1×10^{-3}	17	7.47×10^7	7.48×10^8	18700	10300
2.5×10^{-3}	8.4	3.43×10^7	8.58×10^8		
5×10^{-3}	4.5	1.42×10^7		7780	
1×10^{-2}	3.3	1.40×10^7	8.69×10^8		6800
5×10^{-2}	1.8				6200
0.1	0.9				
0.25	0.8				

[a] The rate coefficient for R = H_2O is referred to as k_0 in the text.

reactions both contribute to the observed decay of 340 nm absorbance:

$$Cl + R \rightarrow \text{products} \qquad (R7)$$

$$Cl_2^- + R \rightarrow \text{products} \qquad (R8)$$

The relative contribution of R7 and R8 to the observed kinetics is determined by the Cl^- concentration and the equilibrium constant for $Cl + Cl^- \rightleftarrows Cl_2^-$. Similar to the studies of background decay of $Cl \rightleftarrows Cl_2^-$ in water, fits of k_R vs [Cl⁻] data to eq 3

$$k_R = \frac{1}{1 + K_3[Cl^-]} k_7 + \frac{K_3[Cl^-]}{1 + K_3[Cl^-]} k_8 \qquad (3)$$

assuming $K_3 = 1.4 \times 10^5$ M^{-1} (see above) give the second-order rate coefficients k_7 and k_8 for the $DMSO_2$ and MS reactions (note that $k'_R \equiv k_R[R] + k'_0$). Plots of k_{DMSO_2} vs [Cl⁻] and k_{MS} vs [Cl⁻] along with fits of the data to eq 3 are shown in Figure 4; values for k_7 and k_8 obtained from these data fits are summarized in Table 2.

Unlike the studies of the $DMSO_2$ and MS reactions, as shown in panel c of Figure 3, the measured second-order reaction rate

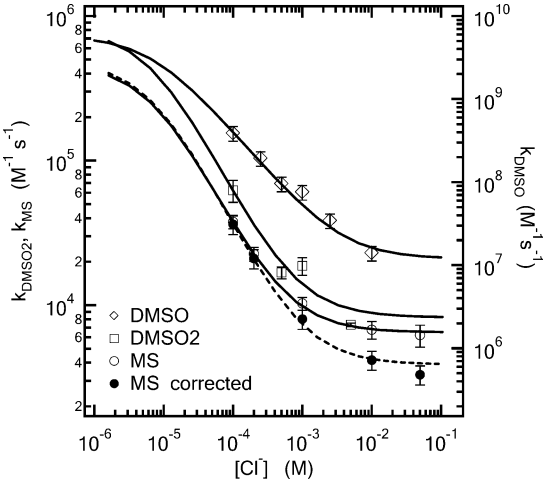

Figure 4. Plot of measured rate coefficients (k_R) for DMSO (◇), DMSO2 (□), and MS (○) reactions as a function of [Cl⁻]. The solid curves are obtained from fitting each set of data to eq 3 in the text. For MS reactions, the dashed curve is for data corrected to the zero ionic strength limit.

coefficient for the MSI reaction is found to be independent of the concentration of Cl^- over the range 10^{-4}−10^{-2} M. The solid line shown in panel c of Figure 3 is obtained from a linear least-squares analysis of all the data shown in the plot; the slope of the solid line gives a value of $(8.2 \pm 0.4) \times 10^8$ M^{-1} s^{-1}, which is very close to an average of the individual rate coefficients measured at each [Cl⁻] (8.25×10^8 M^{-1} s^{-1}). Over the [Cl⁻] range investigated, the fraction of $Cl \rightleftarrows Cl_2^-$ that exists as Cl_2^- at equilibrium varies from ~93% at low [Cl⁻] to >99.9% at high [Cl⁻]. Our results demonstrate that the Cl_2^- + MSI reaction is sufficiently fast that it dominates the observed reactivity at all chloride concentrations investigated. As a result, no information about the kinetics of the Cl + MSI reaction is obtainable from our data. Unfortunately, it is not possible to employ even lower Cl^- concentrations to study the MSI + Cl reaction, because (a) the production rate of $Cl \rightleftarrows Cl_2^-$ radicals from the SO_4^- + Cl^- reaction will be too slow when compared to the decay rate of radicals, which makes it difficult to derive the first-order decay rate of the radicals, and (b) the very fast

TABLE 2: Summary of Kinetics Results for the Reactions of Cl and Cl_2^- with R

		k ($M^{-1} s^{-1}$)		
		this work[a]	lit. value	ref
Cl + R	R = H_2O	$(2.5 \pm 0.4) \times 10^3$	4.5×10^3	40, 47
			2.9×10^3	32, 44
	R = DMSO	$(6.3 \pm 0.6) \times 10^9$	7.0×10^9 [b]	28
	R = DMSO2	$(8.2 \pm 1.6) \times 10^5$		
	R = MS	$(4.9 \pm 0.2) \times 10^5$		
Cl_2^- + R	R = H_2O	< 1.1	24	40, 47
			< 1.8	32
	R = DMSO	$(1.6 \pm 0.8) \times 10^7$	1.2×10^7	27
	R = DMSO2	$(8.2 \pm 5.5) \times 10^3$		
	R = MS	$(3.9 \pm 0.7) \times 10^3$ [c]		
	R = MSI	$(8.0 \pm 1.0) \times 10^8$ [c]		

[a] All uncertainties are 2σ and represent precision of the least-squares analysis of the data. [b] In CCl_4 solvent. [c] Data are corrected to the zero ionic strength limit.

background decay of Cl due to its reaction with H_2O makes it hard to assess the relatively small change in the pseudo-first-order decay rate induced by the reactions of MSI with Cl and Cl_2^-. In summary, the measured rate coefficient of $(8.2 \pm 0.4) \times 10^8$ M^{-1} s^{-1} is attributable to the MSI + Cl_2^- reaction.

Since the reactions of Cl_2^- with MSI and MS both involve two negatively charged reactants, the measured rate coefficients are expected to increase with increasing ionic strength. Furthermore, high concentrations of MS were used because the MS + Cl_2^- reaction is extremely slow. Thus, ionic strength effects are expected to have a major impact on the measurement of the MS + Cl_2^- rate coefficient, but only a very minor impact on the measurement of the MSI + Cl_2^- rate coefficient. In relatively low ionic strength solutions such as those employed in this work (always less than 0.1 M and usually less than 0.01 M), the following relationship is approximately obeyed if both reactants are singly charged:[55]

$$\log k = \log k^0 + \frac{2X\mu^{1/2}}{1 + \mu^{1/2}} \qquad (4)$$

where k is the measured rate coefficient, k^0 is the rate coefficient in the limit of zero ionic strength, μ is the ionic strength

$$\mu = 0.5\sum_i (z_i^2[i]) \qquad (5)$$

where z_i is the charge of species i. In eq 4, X is a collection of physical constants with a value of 0.506 at 295 K in water solvent:[56,57]

$$X = [F^3/4\pi N_A \ln(10)](\rho b^o/2\epsilon^3 R^3 T^3)^{1/2} \qquad (6)$$

where F is the Faraday constant, N_A is Avogadro's number, ρ is the mass density of the solvent, b° is the standard state molality (1 mol kg^{-1}), and ϵ is the permittivity of the solvent.

In the analysis of our data for the MSI and MS reactions, eq 4 was used to convert each measured rate coefficient to an appropriate value for the limit where $\mu \rightarrow 0$. For the MSI reactions, all measured first-order rates were corrected to the zero ionic strength limit using eq 4. However, the data analysis method for MS reactions is not that straightforward. It is worth noting that the rate coefficients for MS + Cl and MS + Cl_2^- both contribute to each measured rate coefficient for MS studies, but the former one is not expected to be significantly dependent on ionic strength under the experimental conditions employed in this study, i.e., we assume that only reactions where both reactants are charged will display significant ionic strength dependences for the rate coefficients in solutions with ionic strengths less than 0.05 M. Hence, the measured pseudo-first-order decay rates for the MS reactions are corrected to the zero ionic strength limit by assuming that k_{MS+Cl} is independent of ionic strength and correcting only k_{MS+Cl_2-}. We used the following iterative method to correct the pseudo-first-order rate from MS + Cl_2^- to the zero ionic strength limit (primed rate coefficients are pseudo-first order and unprimed rate coefficients are second order): (1) linear least-squares analysis of the measured $k'_{MS}{}^{(1)}$ vs [MS] data gives $k_{MS}{}^{(1)}$ (the superscript means iteration i), and $k_{MS+Cl}{}^{(1)}$ and $k_{MS+Cl_2^-}{}^{(1)}$ are obtained by fitting the $k_{MS}{}^{(1)}$ vs [Cl^-] data to eq 4; (2) then corrected values for pseudo-first-order decay rates for MS + Cl and MS + Cl_2^- at each [Cl^-], $k'_{MS+Cl}{}^{(1)}$ and $k'_{MS+Cl_2^-}{}^{(1)}$, are evaluated based on K_3 and $k_{MS+Cl}{}^{(1)}$ and $k_{MS+Cl_2^-}{}^{(1)}$; (3) eq 4 is used to correct $k'_{MS+Cl_2^-}{}^{(1)}$ to the zero ionic strength limit giving $k'_{MS+Cl_2^-(0)}{}^{(1)}$ (the subscript means 0 ionic strength); and (4) the total pseudo-first-order decay rate in the zero ionic strength limit, $k'_{MS(0)}{}^{(2)}$, is calculated from $k_{MS+Cl}{}^{(1)}$ and $k'_{MS+Cl_2^-(0)}{}^{(1)}$, and can be used as the initial input of the next iteration. When the values of k_{MS+Cl} and $k_{MS+Cl_2^-(0)}$ after iteration n differ by less than 2% from those after iteration $n - 1$, they are adopted as the final results for the MS + Cl and MS + Cl_2^- rate coefficients in the zero ionic strength limit.

In Figure 4 the original data (open circles) and those corrected to the zero ionic strength limit (filled circles) for MS reactions are compared. As expected, the differences between the original and the corrected data are evident only on the right side of the plot where the MS + Cl_2^- reaction is dominant in the system, but are negligible on the left side of the plot, where the MS + Cl reaction is more important in determining the measured k_{MS}. As expected, the corrected MS + Cl rate coefficient is very close to the one obtained from the original data, while the corrected rate coefficient for the MS + Cl_2^- reaction in the zero ionic strength limit is about 40% lower than that obtained from the original data. For the very fast MSI reaction, the rate coefficient in the zero ionic strength limit is only about 3% lower than the value obtained from the original data. The kinetic data for the MSI and MS reactions with Cl_2^- listed in Table 1 are corrected to the zero ionic strength limit.

In the studies of DMSO reactions, it was found that the observed pseudo-first-order decay rate, k'_{DMSO}, becomes almost independent of DMSO concentration at high Cl^- concentrations, as typified by the data in panel a of Figure 3 for [Cl^-] = 0.025 M. Two published studies[27,28] have demonstrated that DMSO reactions with both Cl and Cl_2^- lead to the production of the DMSO−Cl adduct, a species that absorbs at 340 nm with an extinction coefficient of ~4000 M^{-1} cm^{-1}, i.e., about half of that for Cl_2^-.[32,37] Therefore the appearance of the DMSO−Cl adduct from both DMSO reactions can contribute to the detected absorbance and interfere with the measurement of the desired rate coefficient. In addition, as the DMSO concentration increases, DMSO consumes an increasing fraction of SO_4^- radicals:

$$SO_4^- + DMSO \rightarrow DMSO^+ + SO_4^{2-} \qquad (R9)$$

Studies of the kinetics of R9 by Kishore and Asmus[58] and by our group[26] agree well and indicate that $k_9 \sim 3.0 \times 10^9$ M^{-1} s^{-1} at room temperature, and Kishore and Asmus[58] have observed the UV absorption spectrum of the product $DMSO^+$. Assuming a rate coefficient of $\sim 3 \times 10^8$ M^{-1} s^{-1} [48,59] for the SO_4^- + Cl^- reaction (R2), it appears that over half of the SO_4^- radicals react with DMSO when [DMSO] = 0.1[Cl^-]. The

$DMSO^+$ radical produced from R9 reacts with Cl^- at a rate close to the diffusion controlled limit to produce the DMSO−Cl adduct:[27]

$$Cl^- + DMSO^+ \rightleftarrows DMSO{-}Cl \quad (R10, R{-}10)$$

Because of the high Cl^- concentration ($\geq 10^{-2}$ M) employed in this study, the equilibrium R10, R−10 facilitates the production of DMSO−Cl, and the production of Cl_2^- is reduced as the DMSO concentration increases. The contribution of DMSO−Cl to the detected absorbance becomes dominant when $[DMSO]/[Cl^-] \geq 0.5$, i.e., more than 80% of SO_4^- reacts with DMSO to produce DMSO−Cl through R9 and R10 without involving Cl_2^- radicals. Under such conditions, the detected absorbance is primarily from DMSO−Cl and the observed absorbance and decay rates cannot be used to derive the $Cl \rightleftarrows Cl_2^-$ + DMSO reaction kinetics. Based on the above analysis, only data obtained for $[Cl^-] < 10^{-2}$ M were fit using eq 3 to obtain rate coefficients for DMSO reactions with Cl and Cl_2^-.

The only available data with which to compare our results are one study each on DMSO + Cl [28] and DMSO + Cl_2^-.[27] Sumiyoshi and Katayama[28] employed a pulse radiolysis method to study the Cl + DMSO reaction in carbon tetrachloride solvent, and report a rate coefficient of $(7.0 \pm 0.5) \times 10^9$ M^{-1} s^{-1}. They also found that the reaction product is the three-electron-bonded DMSO−Cl adduct that possesses an absorption spectrum with a maximum around 400 nm. Kishore and Asmus[27] also used a pulse radiolysis technique and evaluated DMSO + Cl_2^- kinetics in aqueous solution from the pseudo-first-order decay of the absorbance measured at 330 nm in experiments with high $[Cl^-]$ (0.05 M). They report a rate coefficient of $(1.2 \pm 0.2) \times 10^7$ M^{-1} s^{-1} for the DMSO + Cl_2^- reaction, about 25% lower than the value we report here. However, they did not provide important details of the kinetics experiments, i.e., concentrations of DMSO and absorbance decay time scales in their paper. Hence, it is not possible to make informed comments concerning reasons for the relatively small difference in the rate coefficients reported in the two studies.

Spectroscopic Studies of the Aqueous Phase DMSO−Cl Adduct Radical. To obtain a better understanding of the complicated mechanisms involved in our studies of DMSO reactions with $Cl \rightleftarrows Cl_2^-$, especially at high Cl^- concentrations, the absorption spectrum of DMSO−Cl was studied over the wavelength range 320 to 500 nm. All experiments were carried out under conditions where $[Cl^-] = 0.01$ M, $[S_2O_8^{2-}] = (1{-}2) \times 10^{-5}$ M, and the solutions were unbuffered with pH ~5.5. $[DMSO] > 0.6[Cl^-]$ was used to achieve maximum production of DMSO−Cl and minimum Cl_2^- production in the solution since, as discussed above, it was found that the observed absorbance becomes independent of [DMSO] when $[DMSO]/[Cl^-] \geq 0.6$ at a constant $[Cl^-]$, indicating that all SO_4^- reacts with DMSO and produces DMSO−Cl through R9 and R10. By comparing the wavelength dependence of the observed absorbance when DMSO is absent to that when DMSO is present with a concentration $\geq 0.6[Cl^-]$, the absorption spectrum of DMSO−Cl could be derived based on the assumption that the only important loss of SO_4^- radicals in the system is from the reactions with DMSO and Cl^- (i.e., self-reaction and reactions with $S_2O_8^{2-}$, water, or any impurities in the solvent are negligible).

An important factor in determining the DMSO−Cl spectrum is the concentration of Cl^-, which controls the product yield of DMSO−Cl. Due to the equilibrium reactions $Cl^- + DMSO^+ \rightleftarrows$ DMSO−Cl (R10, R−10), $DMSO^+$ and DMSO−Cl radicals coexist in the system after fast decay of SO_4^- via DMSO + SO_4^-, and the fraction of each radical is controlled by $[Cl^-]$. The equilibrium constant (K_{10}) for $DMSO^+ + Cl^- \rightleftarrows$ DMSO−Cl is reported to be 560 M^{-1} at pH ~2.[27] Under the experimental conditions employed in this work, i.e., pH ~5.5, the "effective" K_{10} is found to be reduced to 330 ± 40 M^{-1} because the equilibrium is perturbed by the occurrence of the following two reactions:

$$DMSO^+ + H_2O \rightleftarrows DMSO{-}OH + H^+ \quad (R11, R{-}11)$$

$$DMSO{-}OH \rightarrow CH_3 + CH_3S(O)O^- + H^+ \quad (R12)$$

where the loss of $DMSO^+$ through R11 is driven by the fast nonreversible dissociation[58] of DMSO−OH occurring at a rate of $\sim 10^7$ s^{-1}. Therefore, it is estimated that, after SO_4^- has reacted away, only ~76% of total radicals exist as DMSO−Cl while the remainder exist as $DMSO^+$. The spectrum of $DMSO^+$ is reported as a broad unstructured band[58] with a peak absorbance around 300 nm and a peak extinction coefficient of 1800 M^{-1} cm^{-1}; hence, it is always a very minor contributor to the observed absorbance. Under the assumption that the total radical concentration is determined from the concentration of SO_4^- after the laser flash, i.e., all SO_4^- is converted into either DMSO−Cl or $DMSO^+$, the following expression can be derived:

$$\frac{\epsilon_{DMSO-Cl}}{\epsilon_{SO_4^-}} = \frac{K_{10}[Cl^-] + 1}{K_{10}[Cl^-]} \frac{A_{DMSO-Cl}}{A_0} \quad (7)$$

where A_0 is the maximum absorbance (from SO_4^-) observed after the laser flash when $[DMSO] = [Cl^-] = 0$ and $A_{DMSO-Cl}$ is the analogous absorbance when DMSO and Cl^- are present in the solution with a ratio of >0.6. Then $\epsilon_{DMSO-Cl}$ could be obtained from the observed peak absorbances A_{DMSO} and A_0 as well as the extinction coefficient of SO_4^- at each studied wavelength. The spectrum of SO_4^- has been widely studied before, and since the extinction coefficients from these studies vary by nearly 30%, we have decided to use the average of the three studies by Hayon et al.,[60] Tang et al.,[38] and Yu et al.[32] The reference extinction coefficient for SO_4^- and the obtained $\epsilon_{DMSO-Cl}/\epsilon_{SO_4^-}$ ratio at all wavelengths studied in this work are summarized in Table 3. The DMSO−Cl absorption spectrum

TABLE 3: Reference Extinction Coefficients of SO_4^- and $\epsilon_{DMSO-Cl}/\epsilon_{SO_4^-}$ Ratios Obtained from This Work

wavelength (nm)	$\epsilon_{SO_4^-}$ (M^{-1} cm^{-1})[a]	$\epsilon_{DMSO-Cl}/\epsilon_{SO_4^-}$
320	666	1.8
330	694	2.6
340	730	3.4
350	760	4.3
360	805	5.1
370	865	6.0
380	946	5.9
390	1054	5.5
400	1161	4.8
410	1252	3.9
420	1313	3.3
430	1360	2.7
440	1388	2.3
450	1367	2.0
460	1324	1.8
470	1233	1.6
480	1096	1.6
490	960	1.4
500	805	1.2

[a] Obtained from the average of studies from Hayon et al.,[60] Tang et al.,[38] and Yu et al.;[32] uncertainties are estimated to be ±20%.

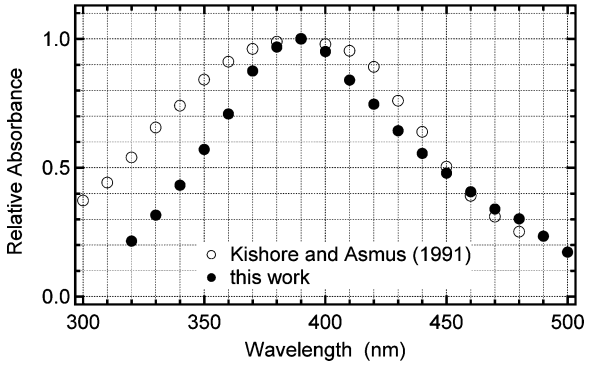

Figure 5. Absorption spectra of the DMSO−Cl adduct from this work (solid circles) and from the study of Kishore and Asmus[27] (open circles).

obtained from the data listed in Table 3 is compared with the spectrum reported by Kishore and Asmus[27] in Figure 5. To accentuate the difference in the shapes of the spectra, peak extinction coefficients are normalized to one. Our DMSO−Cl spectrum has a broad, unstructured band with a maximum absorbance around 390 nm and a peak extinction coefficient of 5760 M^{-1} cm^{-1}; the full-width-at-half-maximum for the spectrum we observe is somewhat narrower than that for the spectrum reported by Kishore and Asmus.[27] Kishore and Asmus[27] used the pulse radiolysis technique and reported the spectrum in the form of $G \times \epsilon$ vs wavelength (G denotes the number of species generated or transformed per 100 eV energy uptake and is approximately 2.8 in their work). They reported a maximum absorbance at 390 nm and estimated a peak extinction coefficient in the range of 5000−7000 M^{-1} cm^{-1}; they also pointed out that this is a typical extinction coefficient range for the structurally similar >S∴X type and other three-electron-bonded radical species.[27,61−63]

Analysis of Systematic Errors. Derivation of rate coefficients for DMSO, $DMSO_2$, and MS reactions with Cl and Cl_2^- employed eq 3, so the equilibrium constant (K_3) for Cl + Cl^- ⇄ Cl_2^- (R3, R−3) is an important parameter in this kinetics study. A value of 1.4×10^5 M^{-1} for K_3 was adopted for all data analyses, based on a collection of studies[32,40,47,50,64] as well as our studies of degradation of Cl ⇄ Cl_2^- in water; the contribution of uncertainties in K_3 to the rate coefficients determined from eq 3 is estimated to be <10%. The loss of Cl and Cl_2^- radicals from reactions with impurities in the samples of Cl^-, $S_2O_8^{2-}$, and sulfur species is another potentially significant source of systematic error. From the very slow decay rate of radicals at high Cl^- concentrations (where Cl_2^- is the dominant radical), reactions of Cl_2^- with impurities in the $S_2O_8^{2-}$ and Cl^- samples are estimated to have an insignificant effect on observed kinetics. The DMSO sample purity was high and the reactions of DMSO with Cl and Cl_2^- are fast, so it is very unlikely that impurity reactions affected the determination of the DMSO rate coefficients. The MS and $DMSO_2$ samples both had stated minimum purities of 98%, and the reactions of these two species with Cl ⇄ Cl_2^- were found to be very slow; hence it cannot be ruled out that the observed kinetics are affected by a minor reactive impurity in the sample (for example, DMSO or MSI). For this reason, the kinetics results obtained for $DMSO_2$ and MS reactions should be strictly considered as upper limits. The MSI sample had a stated minimum purity of ≥97% (impurities unknown). Since MSI is found to be very reactive with Cl_2^-, small amounts of even highly reactive impurities will not noticeably affect the observed kinetics. However, to allow for unidentified systematic errors, we increase the uncertainty somewhat over that due to precision only and report a rate coefficient for the MSI + Cl_2^- reaction of $(8.0 \pm 1.0) \times 10^8$ M^{-1} s^{-1} at 295 K.

In the studies of the DMSO−Cl spectrum, the most significant error comes from uncertainties in the extinction coefficients of SO_4^- adopted as the reference. We used the average of three studies[32,38,60] for the SO_4^- absorption spectrum; uncertainties on $\epsilon_{SO_4^-}$ obtained with this method are estimated to be ∼20%. Other possible sources of systematic error include absorbance ratios listed in Table 3 (<5%), the employment of an effective K_{10} in eq 6 (<5%), and loss of SO_4^- from reactions with background impurities (<5%). Hence, the uncertainty in the extinction coefficients reported in this work is conservatively estimated to be ±30% at all wavelengths where the DMSO−Cl extinction coefficient is more than 10% of its peak value.

Reactivity Trends. The kinetics results from this study show reactivity trends consistent with those obtained from our two previous studies of SO_4^- and OH reactions with organic sulfur compounds,[16,26] as well as other literature studies of the kinetics of aqueous phase radical reactions with organic sulfur compounds. The less oxidized sulfur compounds DMSO and MSI are more reactive toward both Cl and Cl_2^- radicals than the more oxidized sulfur compounds $DMSO_2$ and MS. With the exception of the very reactive (and therefore less selective) species MSI, the Cl radical is more reactive than the Cl_2^- radical by almost 2 orders of magnitude toward the same sulfur compound. This is consistent with the trend observed for Cl ⇄ Cl_2^- reactions with many organic compounds.[65,66]

TABLE 4: Estimated Lifetimes of DMSO, $DMSO_2$, MSIA/MSI, and MSA/MS toward (a) Gas Phase Destruction via Reactions with OH, NO_3, and Cl, (b) Uptake into Aerosols under Remote Tropospheric Conditions, and (c) Aqueous Phase Destruction via Reactions with SO_4^-, OH, Cl, and Cl_2^- Radicals

		τ_x (h)			
process	radical concn[a]	DMSO	$DMSO_2$	MSIA/MSI	MSA/MS
OH(g) + X(g)[b]	1×10^6 cm^{-3}	3−5	>960	3−5	slow
NO_3(g) + X(g)[b]	7×10^6 cm^{-3}	72−240	>18000	fast	slow
Cl(g) + X(g)[b]	5×10^3 cm^{-3}	730	$>2.3 \times 10^6$	fast	slow
X(g) → X(aq)[c]		1−15	1−15	1−15	1−15
SO_4^-(aq) + X(aq)[d]	1×10^{-12} M	0.7	>570	1.2	2.5×10^5
OH(aq) + X(aq)[d]	6×10^{-13} M	0.6	>200	0.5	340
Cl(aq) + X(aq)[d]	1×10^{-13} M	3.5	>27000		45000
Cl_2^-(aq) + X(aq)[d]	1×10^{-11} M	14	>27000	0.3	57000

[a] The radical concentrations refer to the following: global diurnally averaged OH concentration;[71] typical diurnally averaged NO_3 concentration in remote locations;[72] estimated global diurnally averaged Cl concentration;[73,74] Typical diurnally averaged SO_4^-, OH, Cl, and Cl_2^- concentrations in marine boundary layer cloud droplets.[30,31] [b] Gas-phase lifetimes are calculated by using kinetic information from studies by Kukui et al.,[68] Urbanski et al.,[69] Barnes et al.,[75] Hynes and Wine,[76] and Falbe-Hansen et al.[77] [c] Mass transfer is estimated from field observations in the Antarctic troposphere by Jefferson et al.[78] [d] Aqueous phase lifetimes are calculated by using kinetic data from Zhu et al.,[16,26] Flyunt et al.,[23] and this work based on the assumption that marine boundary layer aerosol particles spend about 3 h per day as cloud droplets.[67]

Implications for Atmospheric Chemistry. The implications of the results reported in this study for atmospheric chemistry are summarized in Table 4. Listed in this table are estimated lifetimes of DMSO, $DMSO_2$, MSI, and MSA toward (1) gas-phase destruction via reactions with OH, NO_3, and Cl, (2) uptake into aerosols under remote tropospheric conditions, and (3) aqueous phase destruction via reactions with SO_4^-, OH, Cl, and Cl_2^- radicals at 295 K. All aqueous phase lifetimes were calculated from the rate coefficients obtained in our studies, i.e., this work and two previous studies of OH and SO_4^- kinetics.[16,26] It is worth noting that while the radical concentrations given in Table 4 are reasonable estimates for the specified environments (see footnotes in the table), these concentrations are subject to considerable variability depending upon the average solar zenith angle and the chemical composition of the environment. An important assumption used in the estimation of lifetime of the sulfur species in the condensed phase is that aerosol particles spend only a fraction of their time, estimated to be 3 h per day under marine boundary layer conditions, as aqueous droplets.[67]

OH is the most important radical for oxidizing gas-phase DMSO in the atmosphere. Uptake of DMSO into the condensed phase occurs at about the same rate as OH-initiated gas-phase oxidation, so these processes are both important sinks for gas-phase DMSO. In the aqueous phase, oxidation of DMSO by Cl and OH is so efficient that the lifetime of DMSO in the aqueous phase is estimated to be a few minutes. Hence, gas-phase losses are rate-limiting for DMSO removal from the atmosphere, and the global average lifetime of DMSO can be evaluated by considering the two parallel channels for gas-phase removal; this lifetime is estimated to be 2−4 h. The lifetime of small cloud droplets is similar in magnitude to the DMSO residence time in a droplet, so it is likely that atmospheric DMSO cycles between the gas and condensed phases as cloud droplets go through evaporation/condensation cycles.

MSIA (MSI) is a very reactive intermediate produced during DMS oxidation, and there are no field measurements of atmospheric MSIA (MSI) concentrations available. However, it has been demonstrated in numerous laboratory studies that MSIA/MSI is the primary product from DMSO oxidation by OH radicals in both the gas phase[68,69] and the aqueous phase.[17,19,21] As listed in Table 4, gas-phase MSIA is very short-lived and appears to be oxidized by the OH radical at about the same rate as DMSO.[68] In the aqueous phase, oxidations of MSI by OH, SO_4^-, and Cl_2^- are all very efficient processes for removing MSI from the atmosphere. The oxidation of MSI in the aqueous phase has been proposed to be the primary source of MS;[70] our kinetic result for the MSI + Cl_2^- reaction suggests that this reaction dominates MSI + OH and is the primary removal channel of MSI due to the high concentration of Cl_2^- in marine cloud droplets; the MSI + Cl_2^- reaction appears to account for about 55% of MSI removal while the MSI + OH reaction appears to contribute only ∼30%.

The more oxidized $DMSO_2$ and MS are not as reactive as DMSO or MSIA/MSI in either the gas phase or the condensed phase, so it has been proposed that they are two of the stable end products from atmospheric DMS oxidation, and uptake into condensed phases is the most efficient process to remove them from the gas phase. The data listed in Table 4 suggest that OH is the only important oxidant for $DMSO_2$ and MS, giving a similar lifetime of about 10 days, which is comparable to the typical lifetime of marine aerosols $\tau_{aerosol}$ (∼6 days). Therefore it is quite possible that a significant fraction of $DMSO_2$ and MS is oxidized to produce the more stable product SO_4^{2-} during the particle lifetime toward deposition, particularly under free tropospheric conditions where particle lifetimes are longer than in the boundary layer. In particular, it appears that the OH-initiated oxidation of MS to SO_4^{2-} needs to be properly accounted for to correctly interpret field observations of the MS-to-NSS (non-seasalt sulfate) ratio in atmospheric aerosols. A recent modeling study by von Glasow and Crutzen[70] arrived at the same conclusion.

Acknowledgment. This research was supported by the National Science Foundation through Grant ATM-03-50185. We thank Professor Athanasios Nenes for helpful discussions about cloud processing of aerosols.

References and Notes

(1) Charlson, R. J.; Lovelock, J. E.; Andreae, M. O.; Warren, S. G. *Nature* **1987**, *326*, 655.
(2) Bates, T. S.; Charlson, R. J.; Gammon, R. H. *Nature* **1987**, *329*, 319.
(3) Berresheim, H.; Eisele, F. L. *J. Geophys. Res. Atmos.* **1998**, *103*, 1619.
(4) Ayers, G. P.; Gillett, R. W. *J. Sea Res.* **2000**, *43*, 275.
(5) Davis, D.; Chen, G.; Bandy, A.; Thornton, D.; Eisele, F.; Mauldin, L.; Tanner, D.; Lenschow, D.; Fuelberg, H.; Huebert, B.; Heath, J.; Clarke, A.; Blake, D. *J. Geophys. Res. Atmos.* **1999**, *104*, 5765.
(6) Davis, D.; Chen, G.; Kasibhatla, P.; Jefferson, A.; Tanner, D.; Eisele, F.; Lenschow, D.; Neff, W.; Berresheim, H. *J. Geophys. Res. Atmos.* **1998**, *103*, 1657.
(7) Urbanski, S. P.; Wine, P. H. Chemistry of gas-phase organic sulfur-centered radicals. In *S-Centered Radicals*; Alfassi, Z. B., Ed.; John Wiley and Sons: 1999; pp 97−140.
(8) Jefferson, A.; Eisele, F. L.; Ziemann, P. J.; Weber, R. J.; Marti, J. J.; McMurry, P. H. *J. Geophys. Res. Atmos.* **1997**, *102*, 19021.
(9) Watts, S. F.; Brimblecombe, P. *Environ. Technol. Lett.* **1987**, *8*, 483.
(10) De Bruyn, W. J.; Shorter, J. A.; Davidovits, P.; Worsnop, D. R.; Zahniser, M. S.; Kolb, C. E. *J. Geophys. Res. Atmos.* **1994**, *99*, 16927.
(11) Brimblecombe, P.; Clegg, S. L. *J. Atmos. Chem.* **1988**, *7*, 1.
(12) Watts, S. F.; Brimblecombe, P.; Watson, A. J. *Atmos. Environ.* **1990**, *24*, 353.
(13) Eisele, F. L.; Tanner, D. J. *J. Geophys. Res. Atmos.* **1993**, *98*, 9001.
(14) Sciare, J.; Kanakidou, M.; Mihalopoulos, N. *J. Geophys. Res. Atmos.* **2000**, *105*, 17257.
(15) Harvey, G. R.; Lang, R. F. *Geophys. Res. Lett.* **1986**, *13*, 49.
(16) Zhu, L.; Nicovich, J. M.; Wine, P. H. *Aquat. Sci.* **2003**, *65*, 425.
(17) Meissner, G.; Henglein, A.; Beck, A. G. *Z. Naturforsch. Teil B* **1967**, *22*, 13.
(18) Reuvers, A. P.; Greensto, C.; Borsa, J.; Chapman, J. D. *Int. J. Radiat. Biol.* **1973**, *24*, 533.
(19) Veltwisch, D.; Janata, E.; Asmus, K. D. *J. Chem. Soc., Perkin Trans. 2* **1980**, 146.
(20) Milne, P. L.; Zika, R. G.; Saltzmann, E. S. Rate of reaction of methanesulfonic acid, dimethyl sulfoxide, and dimethyl sulfone with hydroxyl radical in aqueous solution. In *Biogenic Sulfur in the Environment*; Saltzmanm, E. S., Cooper, W. J., Eds.; ACS. Symp. Ser. 393; American Chemical Society: Washington, DC, 1989; pp 518−528.
(21) Bardouki, H.; da Rosa, M. B.; Mihalopoulos, N.; Palm, W. U.; Zetzsch, C. *Atmos. Environ.* **2002**, *36*, 4627.
(22) Sehested, K.; Holcman, J. *Radiat. Phys. Chem.* **1996**, *47*, 357.
(23) Flyunt, R.; Makogon, O.; Schuchmann, M. N.; Asmus, K. D.; von Sonntag, C. *J. Chem. Soc., Perkin Trans. 2* **2001**, 787.
(24) Olson, T. M.; Fessenden, R. W. *J. Phys. Chem.* **1992**, *96*, 3317.
(25) Lind, J.; Eriksen, T. E. *Radiochem. Radioanal. Lett.* **1975**, *21*, 177.
(26) Zhu, L.; Nicovich, J. M.; Wine, P. H. *J. Photochem. Photobio. A* **2003**, *157*, 311.
(27) Kishore, K.; Asmus, K. D. *J. Phys. Chem.* **1991**, *95*, 7233.
(28) Sumiyoshi, T.; Katayama, M. *Chem. Lett.* **1987**, 1125.
(29) Chameides, W. Photochemistry of the atmospheric aqueous phase. In *Chemistry of multiphase atmospheric systems*; Jaeschke, W., Ed.; Springer: Berlin, Germany, 1986; pp 369−414.
(30) Herrmann, H.; Ervens, B.; Jacobi, H. W.; Wolke, R.; Nowacki, P.; Zellner, R. *J. Atmos. Chem.* **2000**, *36*, 231.
(31) Lelieveld, J.; Crutzen, A. P. J. *J. Atmos. Chem.* **1991**, *12*, 229.
(32) Yu, X. Y.; Bao, Z. C.; Barker, J. R. *J. Phys. Chem. A* **2004**, *108*, 295.
(33) Schwarz, H. A.; Dodson, R. W. *J. Phys. Chem.* **1984**, *88*, 3643.
(34) Poskrebyshev, G. A.; Huie, R. E.; Neta, P. *J. Phys. Chem. A* **2003**, *107*, 1964.
(35) Henglein, A. *Radiat. Phys. Chem.* **1980**, *15*, 151.

(36) White, J. U. *J. Opt. Soc. Am.* **1942**, *32*, 285.
(37) Hug, G. L. *Optical Spectra of Nonmetallic Inorganic Transient Species in Aqueous Solutions*; U.S. Department of Commerce: Washington, DC, 1981.
(38) Tang, Y.; Thorn, R. P.; Mauldin, R. L.; Wine, P. H. *J. Photochem. Photobiol. A* **1988**, *44*, 243.
(39) McElroy, W. J.; Waygood, S. J. *J. Chem. Soc., Faraday Trans.* **1990**, *86*, 2557.
(40) McElroy, W. J. *J. Phys. Chem.* **1990**, *94*, 2435.
(41) Bao, Z. C.; Barker, J. R. *J. Phys. Chem.* **1996**, *100*, 9780.
(42) Herrmann, H.; Reese, A.; Zellner, R. *J. Mol. Struct.* **1995**, *348*, 183.
(43) Huie, R. E.; Clifton, C. L.; Altstein, N. *Radiat. Phys. Chem.* **1989**, *33*, 361.
(44) Klaning, U. K.; Wolff, T. *Ber. Bunsen-Ges.* **1985**, *89*, 243.
(45) George, C.; Chovelon, J. M. *Chemosphere* **2002**, *47*, 385.
(46) Buxton, G. V.; Bydder, M.; Salmon, G. A.; Williams, J. E. *Phys. Chem. Chem. Phys.* **2000**, *2*, 237.
(47) Buxton, G. V.; Bydder, M.; Salmon, G. A. *J. Chem. Soc., Faraday Trans.* **1998**, *94*, 653.
(48) Buxton, G. V.; Bydder, M.; Salmon, G. A. *Phys. Chem. Chem. Phys.* **1999**, *1*, 269.
(49) Database, N. N. S. K.: http://kinetics.nist.gov/solution.
(50) Nagarajan, V.; Fessenden, R. W. *J. Phys. Chem.* **1985**, *89*, 2330.
(51) Yu, X. Y.; Barker, J. R. *J. Phys. Chem. A* **2003**, *107*, 1313.
(52) Yu, X. Y.; Barker, J. R. *J. Phys. Chem. A* **2003**, *107*, 1325.
(53) Huie, R. E.; Clifton, C. L. *J. Phys. Chem.* **1990**, *94*, 8561.
(54) Hynes, A. J.; Wine, P. H. *J. Chem. Phys.* **1988**, *89*, 3565.
(55) Espenson, J. H. *Chemical Kinetics and Reaction Mechanisms*; McGraw-Hill: New York, 1981.
(56) Manov, G. G.; Bates, R. G.; Hamer, W. J.; Acree, S. F. *J. Am. Chem. Soc.* **1943**, *65*, 1765.
(57) Atkins, P.; dePaula, J. In *Physical Chemistry*, 7th ed.; W. H. Freeman: New York, 2002; p 261.
(58) Kishore, K.; Asmus, K. D. *J. Chem. Soc., Perkin Trans. 2* **1989**, 2079.
(59) Wine, P. H.; Tang, Y.; Thorn, R. P.; Wells, J. R.; Davis, D. D. *J. Geophys. Res. Atmos.* **1989**, *94*, 1085.
(60) Hayon, E.; Treinin, A.; Wilf, J. *J. Am. Chem. Soc.* **1972**, *94*, 47.
(61) Bonifacic, M.; Asmus, K. D. *J. Chem. Soc., Perkin Trans. 2* **1980**, 758.
(62) Anklam, E.; Asmus, K. D.; Mohan, H. *J. Phys. Org. Chem.* **1990**, *3*, 17.
(63) Anklam, E.; Mohan, H.; Asmus, K. D. *J. Chem. Soc., Perkin Trans. 2* **1988**, 1297.
(64) Jayson, G. G.; Parsons, B. J.; Swallow, A. J. *J. Chem. Soc., Faraday Trans. 1* **1973**, 1597.
(65) Buxton, G. V.; Salmon, G. A. *Prog. React. Kinet. Mech.* **2003**, *28*, 257.
(66) Herrmann, H. *Chem. Rev.* **2003**, *103*, 4691.
(67) Katoshevski, D.; Nenes, A.; Seinfeld, J. H. *J. Aerosol Sci.* **1999**, *30*, 503.
(68) Kukui, A.; Borissenko, D.; Laverdet, G.; Le Bras, G. *J. Phys. Chem. A* **2003**, *107*, 5732.
(69) Urbanski, S. P.; Stickel, R. E.; Wine, P. H. *J. Phys. Chem. A* **1998**, *102*, 10522.
(70) von Glasow, R.; Crutzen, P. J. *Atmos. Chem. Phys.* **2004**, *4*, 589.
(71) Prinn, R. G.; Weiss, R. F.; Miller, B. R.; Huang, J.; Alyea, F. N.; Cunnold, D. M.; Fraser, P. J.; Hartley, D. E.; Simmonds, P. G. *Science* **1995**, *269*, 187.
(72) Noxon, J. F. *J. Geophys. Res.* **1983**, *88*, 1017.
(73) Pszenny, A. A. P.; Keene, W. C.; Jacob, D. J.; Fan, S.; Maben, J. R.; Zetwo, M. P.; Springeryoung, M.; Galloway, J. N. *Geophys. Res. Lett.* **1993**, *20*, 699.
(74) Wingenter, O. W.; Kubo, M. K.; Blake, N. J.; Smith, T. W.; Blake, D. R.; Rowland, F. S. *J. Geophys. Res. Atmos.* **1996**, *101*, 4331.
(75) Barnes, I.; Bastian, V.; Becker, K. H.; Martin, D. *ACS Symp. Ser.* **1989**, *393*, 476.
(76) Hynes, A. J.; Wine, P. H. *J. Atmos. Chem.* **1996**, *24*, 23.
(77) Falbe-Hansen, H.; Sorensen, S.; Jensen, N. R.; Pedersen, T.; Hjorth, J. *Atmos. Environ.* **2000**, *34*, 1543.
(78) Jefferson, A.; Tanner, D. J.; Eisele, F. L.; Davis, D. D.; Chen, G.; Crawford, J.; Huey, J. W.; Torres, A. L.; Berresheim, H. *J. Geophys. Res. Atmos.* **1998**, *103*, 1647.